

# Dynamics of small amplitude, off-resonance AFM

Peter M. Hoffmann

Wayne State University, Department of Physics, Detroit MI 48201, USA

## Abstract

Most current non-contact AFM techniques rely on vibrating the measuring lever at resonance using amplitudes that are large compared to typical interaction length scales. Here we present results of simulations that show that off-resonance, small amplitude AFM provides an alternative non-contact technique in which force gradients can be measured directly without the need of mathematical de-convolution. We show that under a wide range of reasonable conditions the measurements are linear and quantitative.

## Introduction

Atomic resolution Atomic Force Microscopy (AFM) has only been achieved rather recently by using a frequency modulated AFM technique in ultra-high vacuum (UHV) [1-3]. In non-contact AFM (nc-AFM), the accuracy with which the frequency of a high quality factor resonator can be measured allows for the use of stiff cantilevers. This avoids the snap-to-contact instability and makes non-contact atomic resolution imaging possible. Nc-AFM has been very successful and has provided valuable information about interactions between the tip and different atomic sites [4-6], and about atomic energy dissipation [5]. Recently, it has been shown to achieve sub-atomic (orbital) imaging resolution [7]. Because of the large amplitudes used these systems are inherently non-linear. This necessitates mathematical de-convolution of the obtained interaction data (measured as a frequency shift) [8,9]. It also raises questions about the origin of the energy losses in the system [10,11], and how the specific mode of operation and the measuring electronics influence the obtained results [12].

Recently, it has been shown [13,14] that atomic resolution AFM can also be achieved in the amplitude-modulation mode, if a sufficiently sensitive deflection sensor is used. Using a fiber-interferometric sensor [15], sufficiently stiff levers could be used that avoid the instability close to the surface. Moreover, using ultra-small amplitudes of less than 0.25 Å and by operating the instrument far below its first resonance, it was shown that a direct and linear measurement as well as atomic resolution images of the interaction stiffness can be achieved. However, questions remain about the limits of the linearity of the technique, especially with respect to the maximum allowable drive amplitude [16] and frequency. It is also instructive to explore the influence of long- and short-range forces [13] as well as atomic relaxation on the obtained force gradient-distance curves [13,17].

## Theory

In order to set up realistic equations of motion of the vibrating lever, we need to take the different length ranges of tip-surface interactions and the relaxation of tip and surface atoms into account. It is therefore useful to model the system as a number of nodes representing the lever support, the lever, the end of the tip, the surface, and the bulk of the sample. Medium and long-range forces typically contribute very little to the relaxation of the tip since they act on the macroscopic tip structure which has a very high stiffness [13]. However, short-range (e.g. covalent) forces lead to a relaxation of the outermost tip atoms. The relaxation is modelled using constant stiffnesses for the surface and the tip. While this is certainly a simplification, it would be very difficult to include the non-linear stiffness of the relaxing atoms, since this depends on the geometry and chemistry of the surface and tip and

suitable functional forms are not readily available. We thus arrive at the model shown in Figure 1, which leads to the following equations for each node:

$$\begin{aligned}
s_0 &= 0 \\
k_s(s_1 - s_0) + F_{sr}[s_2 - s_1] &= 0 \\
k_t(s_3 - s_2) + F_{sr}[s_2 - s_1] &= 0 \\
m_L \ddot{s}_3 + \gamma_L \dot{s}_3 - k_L(s_4 - s_3) - k_t(s_2 - s_3) - F_{vdW}[s_3 - s_0 + \delta] &= 0 \\
s_4 &= d + A_0 \cos \omega t
\end{aligned} \tag{1a-e}$$

If we define the width of the gap between the outermost atoms at the tip and on the surface as  $\Delta s_{21} = s_2 - s_1$ , we find from equations 1b and 1c:

$$\Delta s_{21} = s_3 + c_{eff} F_{sr}[\Delta s_{21}] \tag{2}$$

where  $c_{eff}$  is the effective compliance of the surface and the tip, given by:

$$c_{eff} = (k_s)^{-1} + (k_t)^{-1} \tag{3}$$

In the following, we assume that the atom at the tip end and the atom at the surface relax very fast, and thus are always in mechanical equilibrium. The gap distance,  $\Delta s_{21}$ , is therefore found by solving equation (2) at every time step of the iteration.

The deflection (amplitude) of the lever, which is the quantity actually measured during an experiment, is given by  $s = s_3 - d$ . Using equations 1a-e we arrive at the following differential equation for the amplitude of the cantilever:

$$m_L \ddot{s} + \gamma_L \dot{s} + k_L s = k_L A_0 \cos \omega t + F_{sr}[\Delta s_{21}] + F_{vdW}[s + d + \delta] \tag{4}$$

where  $\delta$  is a distance describing the size of the nanotip or the offset of the tip end from the macroscopic part of the tip (i.e. that part of the tip that can be described by an overall tip radius,  $R$ ). The parameters  $\delta$  and  $R$  are chosen from actual fits to experimental data.

The functional form of the short-range force used here is taken from a universal interaction energy law obtained from the equation of state for metals [18]. It is given by:

$$F_{sr}[y] = F_{sr}[a(y)] = -\frac{E_b}{\lambda} (a - 0.15a^2 + 0.05a^3) e^{-a} \tag{5}$$

where  $a(y) = y/\lambda$ ,  $E_b$  is the bonding energy, and  $\lambda$  is the length range of the bonding potential.

The van-der-Waals interaction between the tip and the surface depend on the geometry of the tip. From the analysis of experimental data, we found [13] that the long-range force gradients follow approximately a 4<sup>th</sup> degree inverse power law. Since the actual shape of the tip is unknown, the tip can be adequately modelled by a variety of geometries, where the appropriate parameters (tip radius, offset parameter) are determined by experiment. Here, we have chosen a very simple geometry, that of a truncated rod of radius  $R$ . However, a problem arose from the fact that the usual functional form (inverse power law) for the van-der-Waals potential diverges at zero separation. Due to the use of an exponential functional form for the short range potential, and because we allow for atomic relaxation in our model, distances of less than zero can arise in our model. In reality, van-der-Waals forces cannot be described by an inverse power law up to zero separation either, but have to break down once

there is significant orbital overlap and electrons can tunnel between the tip and the surface. We therefore chose a semi-empirical form of the van-der-Waals force, which gives the familiar inverse power law at large distances, but tends towards a constant value as the tip approaches the surface. In addition, by choosing the parameter  $b_0$  judiciously, the short-range and the van-der-Waals force can be smoothly joined. The functional form of the van-der-Waals force used in this paper is:

$$F_{vdW}[x] = -\frac{A_H R^2}{6} \frac{1}{x^3 \left( 1 - \exp\left(\frac{b_0 - x}{b_0}\right) \right) + b_0^3 \exp\left(\frac{b_0 - x}{b_0}\right)} \quad (6)$$

where  $A_H$  is the Hamaker constant (taken to be 2 eV),  $R$  is the tip radius, and  $b_0 = \delta - 1.86144\lambda$ .

In the simulations, we solved equation (4) numerically, obtaining the lever amplitude  $A \equiv s$  and the phase  $\phi$ . For below-resonance operation of the AFM, the measured interaction stiffness is generally given by:

$$k_{tot} = k_L \left( \frac{A_0}{A} (1 - \omega^2 / \omega_0^2)^{-1} \cos \phi - 1 \right) \quad (7)$$

In many cases, however, where  $\omega \ll \omega_0$ , and damping is low, the frequency and the phase terms are very close to 1 and can be omitted. The total measured stiffness is the sum of the short-range and long-range contributions of the interaction. In addition, it is measured versus the *piezo displacement*,  $d$ . Thus, if we want to recover the actual short- and long-range potential, we need to take the bending of the cantilever and the atomic relaxation into account. The bending of the cantilever can be taken into account by combining equations 1c and d in the steady-state case, then taking the derivative with respect to  $d$ , and rearranging to obtain:

$$ds_3 = \left( 1 - \frac{k_{tot}}{k_L} \right)^{-1} dd \quad (8)$$

Integrating over the piezo motion,  $d$ , we can then recover the actual average position of the (macroscopic) tip,  $s_3$ . The short-range contribution of the total interaction stiffness is found by subtracting the van-der-Waals contribution as a function of  $s_3$ :

$$k_m(s_3) = k_{tot}(s_3) - k_{vdW}(s_3) \quad (9)$$

where  $k_{vdW}$  is taken as the derivative of equation (6) with the parameters  $R$  and  $\delta$  determined by a best fit to the long-range tail of the measured interaction stiffness. The tip-surface gap,  $\Delta s_{21}$ , can be found from:

$$d\Delta s_{21} = (1 - c_{eff} k_m) ds_3 \quad (10)$$

The measured short range stiffness,  $k_m$ , consists of the actual short-range interaction stiffness,  $k_{sr}$ , and the tip and surface stiffnesses,  $k_s$  and  $k_t$ , here represented by the compliance  $c_{eff}$ . Since  $k_t$ ,  $k_s$  and  $k_{sr}$  are springs in series, we find:

$$k_{sr} = \frac{k_m}{1 - c_{eff} k_m} \quad (11)$$

## Results

Figure 2 shows simulated force gradient curves in the case where only short-range forces are present and the tip/surface relaxation is low ( $k_t, k_s = 1000$  N/m or  $c_{eff} = 0.02$  Å/nN). The short range force parameters are  $E_0=3.4$  eV and  $\lambda = 0.54$  Å which are modelled after actual measurements of interactions between a W tip and a reconstructed Si(111) surface in UHV [13]. Shown are curves for different lever amplitudes from 0.1 Å to 1Å. The applied frequency was 100 Hz in all cases (resonance frequency of the lever: 16.2 kHz). It can be seen that up to an amplitude of 0.25 Å the measurement is essentially error-free, at 0.5 Å small errors start to appear, and at 1Å the error is quite large. This emphasizes the need for small amplitudes if linear and accurate measurements are desired. In actual experiments, we have used amplitudes of 0.13 - 0.25 Å [13,14]. The desirable amplitude range depends, of course, on the actual shape of the force curve, but it is probably safe to say that in the measurement of atomic bonding curves, amplitudes of less than 0.25 Å are necessary if accurate measurements are to be achieved.

Figure 3 shows a set of simulations at 0.1 Å amplitude under similar conditions, but at different applied frequencies, analysed using equation (9). As the frequency is increased, the free amplitude of the lever increases due to resonance enhancement. However, this effect is included in the frequency term of equation (6) and as can be seen in Figure 2, relatively high frequencies can be used without too much distortion in the final measurement. It can be seen that up to a few kHz ( $< 1/3$  resonance frequency), the measurement is essentially unaffected, however at 5 KHz some distortions of the force gradient curve become visible.

We have shown so far that given suitable operational parameters, small amplitude, off-resonance AFM provides a direct and precise measurement of the interaction stiffness. As a rule of thumb, suitable parameters are amplitudes  $A_0 < \frac{1}{2} \lambda$  and frequencies  $\omega < 1/3 \omega_0$ . In the case of atomic bonding interactions this translates into  $A_0 < 0.25$  Å. We are now routinely using  $A_0 < 0.15$  Å in our experiments [19].

A more general question remains to be answered: How well can we reconstruct the actual short-range bonding interaction between the tip and the surface in the presence of significant relaxation and long-range forces. In practice it is very difficult, since we do not know the actual shape of the long-range interaction and the relaxation potential of the tip and surface atoms. Experimentally it is found that the long-range tail of the measured force or force gradient curve can be modelled quite well by a suitable inverse power law [4,13]. This usually involves two adjustable parameters, a tip radius (or other geometric factor), and a distance offset. We have found that the particular choice of these parameters (and the modelled tip geometry) does not affect the final analysis unduly, since they are constrained by the experimental data. However, as discussed above, it is not clear how these long-range terms behave at very small distances, since they diverge at zero separation.

Even if we know exactly what the functional form and the respective parameters are, as we do in the case of a simulation, we have found that due to the finite number of data-points, the actual short-range interaction can not be completely reconstructed. This is a general problem, independent of the particular AFM technique used. In Figure 4, we show the step-by-step reconstruction of the short-range component of the interaction stiffness and compare it to the shape of the curve that was originally entered into the simulation. It can be seen that the reconstructed curve is quite close to the theoretical one, but that deviations become increasingly apparent as the surface is approached. This is most likely due to cumulative errors in replacing integrals of equations (7) and (9) by finite summations over discrete data points.



## Figure Captions

Figure 1: Schematic of the model that describes lever motion in the presence of long- and short-range interactions, as well as tip and surface relaxation. On the left is a schematic of the AFM setup (not to scale), and on the right are corresponding elements used in the analysis of the mechanics of the system. For more details see text.

Figure 2: Simulated interaction stiffness curves for different applied lever amplitudes. Only short-range interactions were considered with  $\lambda = 0.54 \text{ \AA}$  and  $E_b = 3.4 \text{ eV}$ . The lever frequency was set to 100 Hz (lever resonance 16.9 kHz).

Figure 3: Simulated interaction stiffness curves for different lever frequencies. Amplitude is  $0.1 \text{ \AA}$  for all curves. Only short-range interactions were considered (parameters see Fig. 1).

Figure 4: Simulated interaction stiffness curve ( $k_{\text{tot}}$ ) and subsequent analysis steps. Step 1: Correct for bending of cantilever, Step 2: Subtract long-range background, Step 3: Correct for relaxation of tip atoms due to short-range interaction. Short-range parameters are the same as Figs. 1 and 2. Long-range parameters are  $R = 100 \text{ \AA}$  and  $\delta = 11 \text{ \AA}$ . Frequency was 100 Hz and amplitude  $0.1 \text{ \AA}$ . It can be seen that the original short-range curve ( $k_{\text{sr}}$ , theoretical) can be approximately recovered, but due to the replacement of integrals with summations in rescaling the axes, errors appear. For more details see text.

## References

1. H. Ueyama, M. Ohta, Y. Sugawara, S. Morita, *Jpn. J. Appl. Phys. Part 2*, 34 (1995) L1086-1088.
2. S. Kitamura, M. Iwatsuki, *Jpn. J. Appl. Phys., Part 2*, 34 (1995) L145-L148.
3. F. J. Giessibl, *Science* 267 (1995) 68-71.
4. M. Guggisberg, M. Bammerlin, Ch. Loppacher, O. Pfeiffer, A. Abdurixit, V. Barwich, R. Bennewitz, A. Baratoff, E. Meyer, H.-J. Güntherodt, *Phys. Rev. B* 61 (2000) 11151-11155.
5. B. Gotsmann, H. Fuchs, *Phys. Rev. Lett.* 86 (2001) 2597-2600.
6. H. Hölscher, A. Schwarz, W. Allers, U. D. Schwarz, R. Wiesendanger, *Phys. Rev. B* 61 (2000) 12678- 12681.
7. F. J. Giessibl, H. Bielefeldt, S. Hembacher, J. Mannhart, *Ann. Phys.* 10 (2001) 887-910.
8. F. J. Giessibl, *Phys. Rev. B* 56 (1997) 16010-16015.
9. U. Dürig, *New J. Phys.* 2 (2000) 5.1-5.12.
10. M. Gauthier, M. Tsukada, *Phys. Rev. Lett.* 85 (2000) 5348-5351.
11. N. Sasaki, M. Tsukada, *Jpn. J. Appl. Phys.* 39 (2000) L1334-L1337.
12. M. Gauthier, N. Sasaki, M. Tsukada, *Phys. Rev. B* 64 (2001) 085409.
13. P. M. Hoffmann, A. Oral, R. A. Grimble, H. Ö. Özer, S. Jeffery, J. B. Pethica, *Proc. R. Soc. Lond. A* 457 (2001) 1161-1174.
14. A. Oral, R. A. Grimble, H. Ö. Özer, P. M. Hoffmann, J. B. Pethica, *Appl. Phys. Lett.* 79 (2001) 1915-1917.
15. D. Rugar, H.J. Mamin, P. Guethner, *Appl. Phys. Lett.* 55 (1989) 2588-2590.
16. H. Hölscher, U.D. Schwarz, and R. Wiesendanger, *Appl. Surf. Sci.* 140 (1999) 344.
17. R. Pérez, I. Štich, M. C. Payne, and K. Terakura, *Phys. Rev. B* 58 (1998) 10835-10849.
18. J. H. Rose, J. R. Smith, F. Guinea, J. Ferrante, *Phys. Rev. B* 29 (1984) 2963–2969.
19. P. M. Hoffmann, S. Jeffery, J. B. Pethica, H. Ö. Özer, A. Oral, *Phys. Rev. Lett.* 87 (2001) 265502.

Figure 1

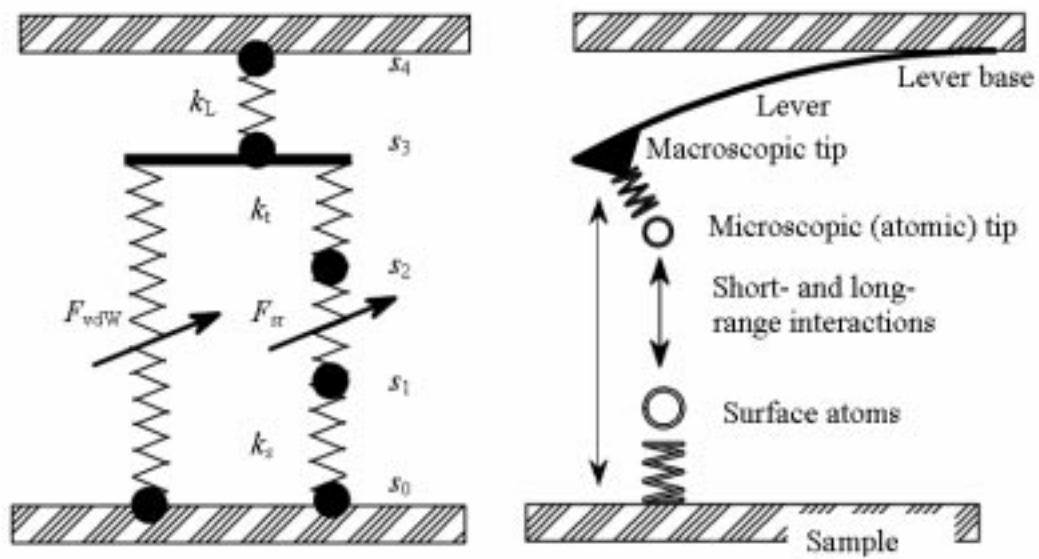


Figure 2

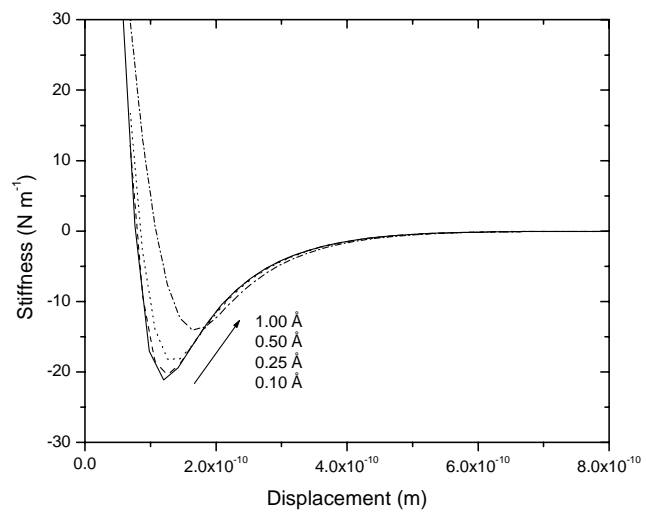


Figure 3

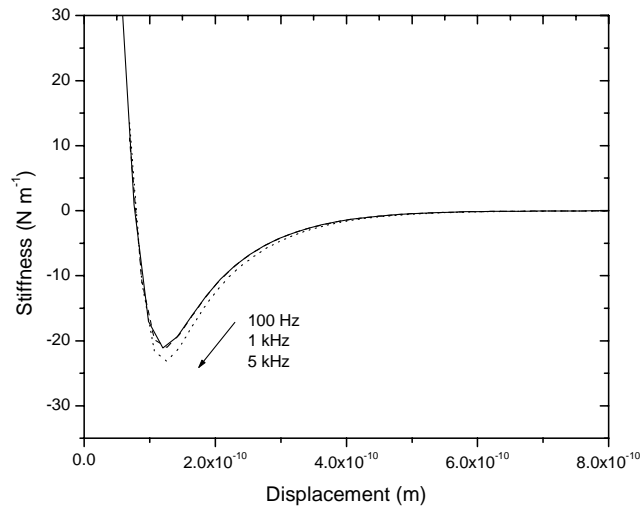


Figure 4

